This article was downloaded by:
On: *14 January 2011*
Access details: *Access Details: Free Access*
Publisher *Taylor & Francis*
Informa Ltd Registered in England and Wales Registered Number: 1072954 Registered office: Mortimer House, 37-41 Mortimer Street, London W1T 3JH, UK

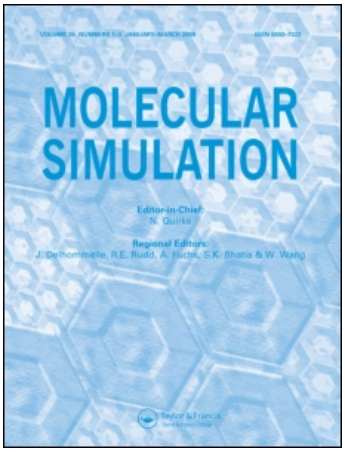

Molecular Simulation
Publication details, including instructions for authors and subscription information:
http://www.informaworld.com/smpp/title~content=t713644482

Nanotube-polymer composites: insights from Flory-Huggins theory and mesoscale simulations

Amitesh Maiti[a]; James Wescott[b]; Paul Kung[a]
[a] Accelrys Inc., San Diego, CA, USA [b] ‡Accelrys Inc., Cambridge, UK

To cite this Article Maiti, Amitesh , Wescott, James and Kung, Paul(2005) 'Nanotube-polymer composites: insights from Flory-Huggins theory and mesoscale simulations', Molecular Simulation, 31: 2, 143 — 149
To link to this Article: DOI: 10.1080/08927020412331308539
URL: http://dx.doi.org/10.1080/08927020412331308539

PLEASE SCROLL DOWN FOR ARTICLE

Full terms and conditions of use: http://www.informaworld.com/terms-and-conditions-of-access.pdf

This article may be used for research, teaching and private study purposes. Any substantial or systematic reproduction, re-distribution, re-selling, loan or sub-licensing, systematic supply or distribution in any form to anyone is expressly forbidden.

The publisher does not give any warranty express or implied or make any representation that the contents will be complete or accurate or up to date. The accuracy of any instructions, formulae and drug doses should be independently verified with primary sources. The publisher shall not be liable for any loss, actions, claims, proceedings, demand or costs or damages whatsoever or howsoever caused arising directly or indirectly in connection with or arising out of the use of this material.

Molecular Simulation, Vol. 31, No. 2–3, 15 February–15 March 2005, 143–149

Taylor & Francis
Taylor & Francis Group

Nanotube–polymer composites: insights from Flory–Huggins theory and mesoscale simulations

AMITESH MAITI*†, JAMES WESCOTT‡ and PAUL KUNG†

†Accelrys Inc., 9685 Scranton Road, San Diego, CA 92121, USA
‡Accelrys Inc., 334 Cambridge Science Park, Cambridge, UK

(Received April 2004; in final form April 2004)

Carbon nanotube (CNT)-polymer composites, with potential applications in structural materials, optoelectronics, sensors, biocatalysis, and thermal and electromagnetic shielding are an important emerging area of nanotechnology. However, progress has been slow due to difficulties in dispersing CNTs into the polymer matrix. We attack the problem from a Flory-Huggins theory point of view, and present novel simulations of the dispersion process at the mesoscale. The solubility parameter of the CNTs is mapped out as a function of tube diameter, and compared with that of well-known polymers. Parallel alignment of CNTs with the application of shear, and dispersion by attaching organic functional groups are also investigated.

Keywords: Nanotubes; Nanocomposites; Mesoscale; Flory-Huggins; DPD

Downloaded At: 18:26 14 January 2011

1. Introduction

Extraordinary mechanical, elastic, thermal, and electrical properties of carbon nanotubes (CNTs) have prompted the design of novel composite materials in which CNTs are dispersed within polymeric matrices [1,2]. Applications can range from structural materials, to electromagnetic and heat shielding, to optoelectronics, to thin films for biocatalysis and gas sensing. Performance depends on several factors, including dispersion uniformity and degree of parallel alignment of CNTs, and the strength of CNT-polymer bonding. Since it is difficult to control many of these properties experimentally, modeling and simulations could provide crucial insights by studying variation of composite morphology as a function of CNT diameter, chirality, and structural modification/functionalization.

There have been several atomic-scale investigations of the interaction between polymer and an isolated nanotube using analytical continuum mechanics [3,4], classical forcefields [5–7], reactive potentials [8–11], etc. Although these simulations yield useful insights, they are not suitable for exploring the overall morphology at length-scales most relevant to nanocomposites, i.e. tens of nanometers (nm) to microns. The biggest challenge for an atomistic approach lies not only in the significant number of particles involved, but also in simulating over equilibration times that are orders of magnitude longer than a nanosecond, a typical limit of classical molecular dynamics (MD) simulations. One way to circumvent this problem is to use a mesoscale modeling technique, which extends simulation limits to length and time-scales appropriate to the study of CNT-polymer nanocomposites. Mesoscale modeling has been successfully used in the study of polymer-melts, polymers in solution, and phase equilibrium of liquid–liquid mixtures. This paper represents a first attempt of applying such method to the study of CNT-polymer composites.

2. Mesoscale method: Dissipative Particle Dynamics

Several flavors of mesoscale modeling exist in the literature. Accelrys Materials Studio suite of software incorporates two distinct methods — a particle-based method called Dissipative Particle Dynamics (DPD), and a density-based method called Mesodyn. Our overall strategy for investigating a CNT-polymer composite consists of (1) determining the equilibrium morphology of the nanotube-polymer system using DPD; (2) using the density map from (1) as an input to a finite-elements program to compute useful materials properties for

*Corresponding author. E-mail: amaiti@accelrys.com

Molecular Simulation
ISSN 0892-7022 print/ISSN 1029-0435 online © 2005 Taylor & Francis Group Ltd
http://www.tandf.co.uk/journals
DOI: 10.1080/08927020412331308539

the composite. In this paper, we describe only our initial DPD simulations and step (2) is left to future work.

In DPD [12] one represents an entire functional group by a single bead, thereby substantially reducing the number of particles to be simulated. The positions and velocities of the spherical beads are propagated by standard integrators as in regular MD methods and thermally equilibrated through a Langevin thermostat. But rather than interact through Lennard-Jones forces, the beads feel a simple soft pair-wise conservative potential which embodies the essential chemistry of the system, and determines whether or not the CNTs disperse in a given polymer. This force is short range and has a simple analytic form resulting in fast computation per time-step. More importantly it provides an effective time-step of several picoseconds, 3–4 orders of magnitude larger than typical time-steps employed in a MD simulation. Details of the equations describing bead–bead interactions in DPD, and extra terms necessitated by the high stiffness of CNTs are relegated to the Appendix.

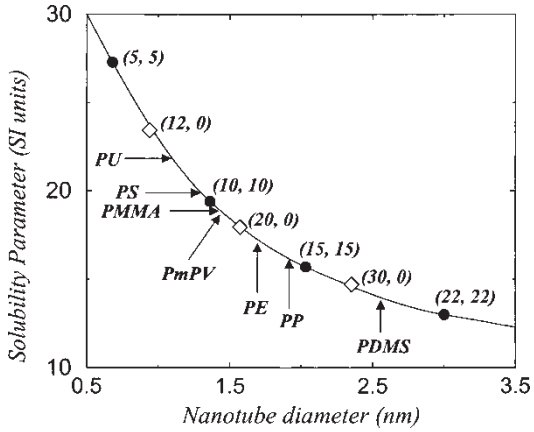

Figure. 1. Plot of calculated solubility parameter (δ) (in units of $(J/cm^3)^{1/2}$) versus tube diameter for armchair (filled circles) and zigzag (unfilled diamonds) CNTs. The published [18] solubility values for poly(urethane) (PU), poly(styrene) (PS), poly(methylmethacrylate) (PMMA), poly(m-phenylenevinylene) (PmPV), polyethylene (PE), polypropylene (PP) and poly(dimethylsiloxane) (PDMS) are also indicated on the plot for comparison.

3. Flory-Huggins theory and solubility parameters

The chemistry of polymer-nanotube interaction is incorporated through relating the DPD bead-bead repulsion to the Flory-Huggins χ-parameter [12]. The Flory-Huggins approach is well known in its application to the equilibrium thermodynamics of polymer solutions [13,14]. In order to determine the χ-parameter, we followed the simple scheme of squaring the difference of pure-component Hildebrand solubility parameters (δ) [15–17], defined as the square root of the cohesive energy density. Strictly speaking, this approach is equivalent to considering only the enthalpic contribution to the χ-parameter, χ_H. In polymer-solvent systems the entropic component χ_S ($= \chi - \chi_H$) is assigned a value between 0.3 and 0.4 (typically 0.34), but in the absence of any reasonable estimate for the contribution of χ_S in polymer-nanotube composite systems we have chosen not to include this.

The solubility parameters of polymers depend to some degree on the length of polymer chains and the method of synthesis, but reliable average values of δ for long-chain polymers can be estimated from simple correlation methods based on fitting a large amount of experimental data[†] [18]. On the other hand, carbon nanotubes are not polymers in the conventional sense, and therefore, their solubility parameters have not previously been investigated. Nevertheless, since CNTs tend to form close-packed bundles, a good measure of their cohesive energy can be obtained from the debundling energy, *i.e.* the energy cost of isolating a CNT from a bundle. Computing such energy with the Universal Forcefield [19] normalizing per unit volume, and taking the square root results in a solubility parameter that is essentially independent of the CNT chiral angle, and that decreases smoothly as a function of the CNT diameter, as displayed in figure 1. The graph in figure 1 also indicates the relative positions of some common polymers on the solubility scale. Flory-Huggins theory predicts that components with small χ (which leads to small DPD repulsion parameter) should mix, while components with χ greater than a critical value, χ^c, should segregate. Since in our analysis χ is based entirely on the differences in Hildebrand solubility parameters it is predicted from figure 1 that PMMA polymers should mix well with CNTs of diameters close to 1.4 nm (*e.g.* (10, 10) CNTs), while PP is expected to form uniform composites with CNTs of diameters in the neighborhood of 1.9 nm (*e.g.* (15, 15) CNTs). For comparison, we have also computed the CNT solubility parameters (δ) with the DREIDING [20] and the COMPASS [21] forcefields, and the results were very similar both qualitatively and quantitatively. Thus for each Forcefield, δ decreased approximately as inverse square-root of the tube-diameter, and for the (10, 10) tube the computed δ (in units of $(J/cm^3)^{1/2}$) were 19.36 (UFF), 18.25 (DREIDING), and 18.89 (COMPASS), respectively. The UFF, DREIDING and COMPASS have all been used to study properties of CNT systems, including computation of Young's modulus (UFF) [22], to investigating mechanical collapse under hydrostatic pressure (DREIDING) [23], to studying CNT-polymer binding interactions (COMPASS) [24].

The applicability of Flory-Huggins theory to CNT-polymer composites, and the accuracy of the CNT δ-values of figure 1 can only be justified by careful experiments. We are aware of one such experiment on CNT-Poly(m-phenylenevinylene) (PmPV) composites [25], where one observes selective affinity of the PmPV polymer ($\delta \sim 18.5\,(J/cm^3)^{1/2}$) to CNTs of diameters ranging between 1.35 and 1.55 nm. This provided strong

[†]http://www.accelrys.com/cerius2/synthia.html.

Downloaded At: 18:26 14 January 2011

justification for using the δ-parameters of figure 1 to perform DPD simulations on CNT-polymer nanocomposites, and gain useful information on the composite morphology. It is also to be noted that the δ's in figure 1 are consistent with strong hydrophobicity known for all CNTs (Note: $\delta_{water} \sim 47.9\,(J/cm^3)^{1/2}$ [26,27]).

4. Results from DPD simulations

Although figure 1 provides an initial screening of which polymers blend with CNTs of given diameters, it is still necessary to perform explicit DPD simulations to address important questions relating to the degree of dispersion, time-scales associated with the dispersion process, effectiveness and critical concentration of specific functional groups in solubilizing CNTs, effect of creating covalent bonds between CNTs and polymer, and to apply external constraints such as the imposition of shear, that can be used to align CNTs in the composite. For the initial set of DPD simulations we chose PMMA ($\delta \sim 19.0$) as a concrete example, because it is a popular polymer used in experimental studies of nanocomposites [28–33]. The original DPD code [12] uses simple spring potentials to represent polymeric chains. We introduced an additional spring and an angle-dependent interaction between CNT-beads in order to mimic the structural rigidity of nanotubes (see Appendix). We studied several nanotubes, but report only the most salient results for $(10, 10)$ and $(15, 15)$ CNTs. In all these studies the relative amount of the CNTs in the composite was fixed at 5% in volume fraction, and the equilibrium morphology was obtained following a total simulation of 5×10^5 steps, corresponding to a real time of $\sim 9\,\mu s$.

Figure 2 displays results for a PMMA composite with $(10, 10)$ CNTs. As expected, the $(10, 10)$ CNTs readily mix with PMMA (figure 2(a)), with the CNTs randomly oriented within the polymer matrix. For mechanical properties, such as the elastic modulus, a more parallel alignment of the CNTs would be desirable. Borrowing from known experimental procedure [34] we subjected the morphology in figure 2(a) to shearing forces‡ [35], which resulted in the morphology of figure 2(b).

Figure 3 displays the results for $(15, 15)$ CNTs. The unfunctionalized $(15, 15)$ CNTs appear immiscible with PMMA, and segregate. Possible strategies to effectively disperse CNTs into immiscible solvents, including polymers, could be: (1) functionalizing the CNTs by covalently attaching compatibilizing groups (schematically shown in figure 3(b) inset); (2) coating the CNTs with appropriate surfactants; (3) modifying the polymer with appropriate groups/blends, and so on. Figure 3(b) displays the resulting morphology upon attaching PMMA monomer groups to the $(15, 15)$ CNT (strategy (1) above) at a relative volume fraction of 30%.

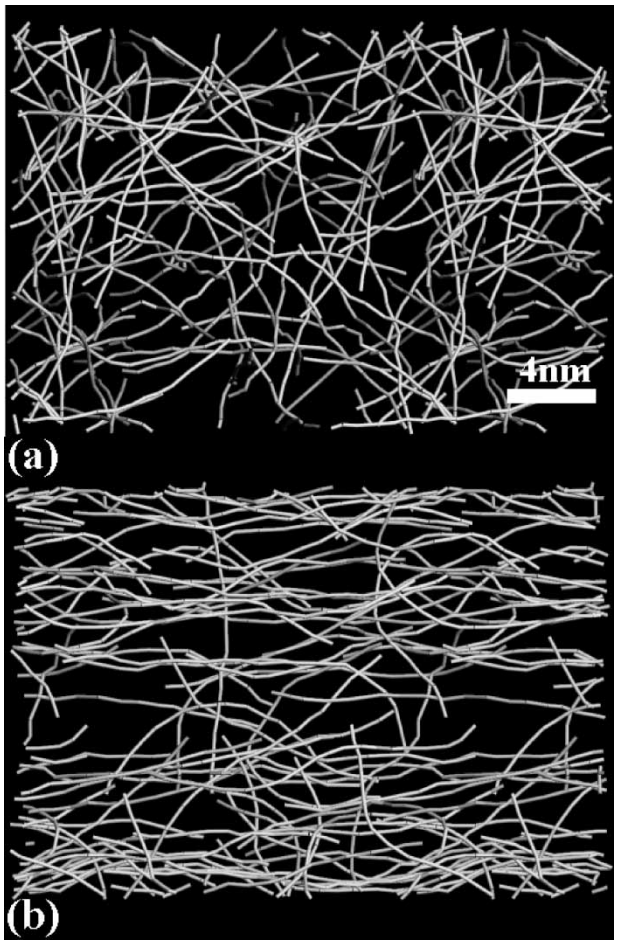

Figure 2. Equilibrium morphologies of $(10, 10)$ CNT-PMMA composites at ambient temperature and pressure as modeled by DPD. (a) Dispersed CNTs; (b) parallel alignment during application of shear. CNTs are shown in white while the PMMA chains are hidden for clarity. Note: each CNT is represented as a string of beads, but string thickness does not reflect physical diameter of a CNT.

It should be mentioned here that although we use a CNT-diameter-dependent solubility parameter in order to compute the CNT-polymer interactions, we physically represent nanotubes as a string of DPD "beads" as a first approximation. Our model does not consider real physical tubes with empty volumes inside, which, depending on the nanotube diameter may or may not be accessible to polymers. Assuming that the inner cavity of a CNT is not accessible to the polymer (as would be true for a narrow-diameter tube), one could attempt to incorporate finite CNT-diameter effects through a combination of smaller (and diameter-dependent) values of r_{ij}^0 for the CNT-spring term (see Appendix) and a larger interaction cutoff for the CNT-beads. We believe that these details will not significantly affect the main conclusions regarding CNT-polymer miscibility except when χ is quite close to its critical value, but could become important in computing physical properties of the nanocomposite, where we would

‡The simulations in figure 2(b) applied a default shear rate of 0.2 DPD units, to quickly generate a typically sheared morphology. For our choice of beads, this shear rate physically corresponds to ~ 9 MPa/ns.

Downloaded At: 18:26 14 January 2011

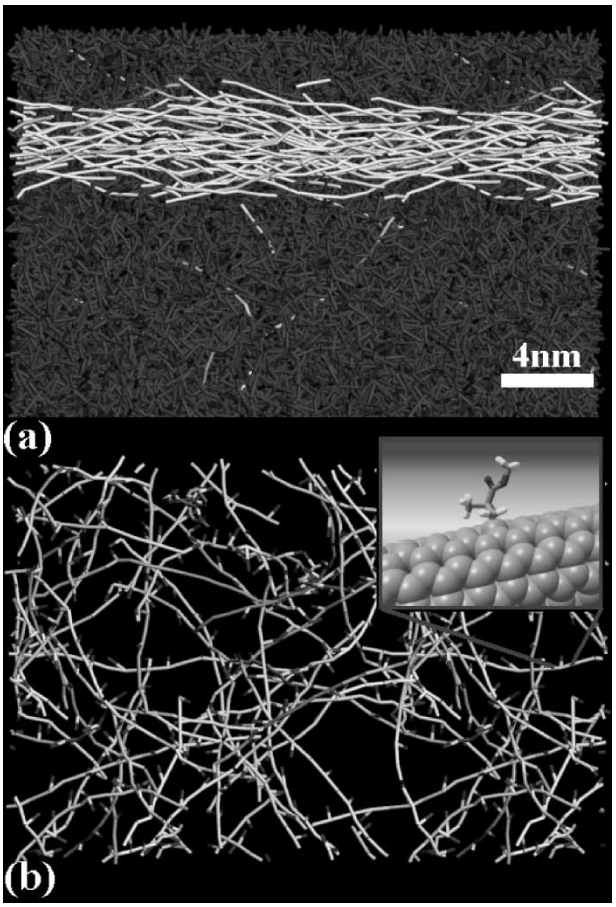

Figure 3. Equilibrium morphologies of (15, 15) CNT-PMMA composites at ambient temperature and pressure as modeled by DPD. CNTs are shown in white in both images. In (a) the PMMA chains are shown in red while in (b) they are hidden for clarity. (a) Unfunctionalized (15, 15) CNTs which quickly segregate and align. (b) Dispersion of (15, 15) CNTs functionalized with 30% (by volume) acrylate groups attached at regular intervals (shown in red). (b-inset) An atomistic representation of one of the acrylate groups attached to a CNT.

Downloaded At: 18:26 14 January 2011

wish the density fields generated to more accurately reflect the real volume of the tube.

5. Future directions and summary

A more exhaustive study on the effect of CNT and polymer lengths, temperature, relative composition, shear rate, and fraction, position, and chemical structure of attached groups is currently planned. Also worth exploring are other mixing strategies, because functionalizing CNTs can often be challenging experimentally. Finally, we note that the equilibrium morphology obtained from DPD simulations could be used as input for finite-element-based approaches [36,37] allowing the calculation of mechanical, electrical, and thermal properties of the nanocomposite.

In summary, using mesoscale methods we have extended simulations on polymer-nanotube composites to time and length-scales of direct relevance to experimentalists, which are orders of magnitude larger than possible with classical MD simulations. In the process, we have, for the first time, mapped out the solubility parameter of the CNTs as a function of the CNT-diameter, which provides a fast screening tool for the choice of an appropriate polymer for a composite. Results presented here position mesoscale modeling as a practical and powerful tool that should generate new interest and lead to further progress in the field of CNT-polymer nanocomposites.

Acknowledgements

We would like to thank Accelrys Inc. for its support of this research. We would also like to acknowledge useful discussions with Simon McGrother, Gerhard Goldbeck-Wood, and Scott Kahn.

Appendix: DPD theory—basic equations revisited

In the DPD formalism, the beads simply follow Newton's equations of motion:

$$\frac{\mathrm{d}\vec{r}_i}{\mathrm{d}t} = \vec{v}_i; \quad \frac{\mathrm{d}\vec{v}_i}{\mathrm{d}t} = \vec{f}_i,$$

where all the masses are normalized to 1 for simplicity, and the force $\vec{f}_i$ on bead i contains three parts, each of which is pairwise additive:

$$\vec{f}_i = \sum_j{}' \left(\vec{f}_{ij}^{\,\mathrm{c}} + \vec{f}_{ij}^{\,\mathrm{D}} + \vec{f}_{ij}^{\,\mathrm{R}}\right)$$

where $\sum_j'$ denotes summation over index j with $i = j$ excluded. In the above equation, f^{D} and f^{R} are respectively, the dissipative and random forces, which effectively act as a thermostat and result in fast equilibration to the Gibbs-Boltzmann canonical ensemble. The significance of these terms is investigated in detail elsewhere [38] and will not be discussed further in this paper. Instead, we focus on $\vec{f}_{ij}^{\,\mathrm{c}}$, which is modeled as a soft repulsion between beads i and j. The force acts along the line joining the two beads, and is therefore conservative (i.e. momentum conserving). Groot and Warren [12] assumed the following functional form for f^{c}:

$$f_{ij}^{\mathrm{c}}(\vec{r}) = a_{ij}\left(1 - r/R_{\mathrm{c}}\right), \quad |\vec{r}| = r \le R_{\mathrm{c}}$$

$$= 0, \quad r > R_{\mathrm{c}}$$

The parameters a_{ij}, henceforth referred to as *bead–bead repulsion parameters*, or simply as *DPD interaction parameters*, depend on the underlying atomistic interactions. The interaction range R_{c} in the above equation sets the basic length-scale of the system, and is defined as the side of a cube containing an average number of $\bar{\rho}$ beads. Therefore, $R_{\mathrm{c}} = (\bar{\rho}V_{\mathrm{b}})^{1/3}$, where V_{b} is the volume of a bead. One can think of $\bar{\rho}$ as a *dimensionless bead-density*, related to the average bead-density $\rho = 1/V_{\mathrm{b}}$ by the equation $\bar{\rho} = \rho R_{\mathrm{c}}^3$. Even in a heterogeneous system consisting of several different species, the basic assumption is that all bead-types (each representing a single

species) are of the same volume V_b. This assumption is useful in order to conform to the Flory-Huggins χ-parameter theory.

Let us now focus on the DPD interaction parameters. The Accelrys DPD code[¶] works with interaction parameters in reduced (i.e. dimensionless) units $\bar{a} = aR_c/kT$, and that's the convention we follow here. If one assumes the same bead-density for all components, one can show [15] that the intra-species interaction parameters are the same for all species, i.e.

$$\bar{a}_{AA} = \bar{a}_{BB}$$

for all species A and B. Therefore, it is the cross-species interaction $\bar{a}_{AB}$, or to be more precise, the excess interaction $\Delta\bar{a} = (\bar{a}_{AB} - \bar{a}_{AA})$ that determines whether components A and B will mix or segregate. The situation is quite similar to the well-known Flory-Huggins theory of polymers in solutions where the χ-parameter controls mixing or segregation behavior. It is therefore only natural to seek a relationship between $\Delta\bar{a}$ and the Flory-Huggins χ-parameter. For a homogeneous mixture it can be shown that [12,15]:

$$\chi_{AB} = 2\alpha\bar{\rho}\Delta\bar{a},$$

where $\alpha \sim 0.1$ is roughly a constant. However, for a segregated mixture the above relation does not hold. Using the computed volume fraction of the minority component in the homogeneous part of the mixture, Groot-Warren (GW) determined a linear fit [12] for a monomer–monomer mixture:

$$\chi \approx 0.286\Delta\bar{a}\,(\text{for}\,\bar{\rho} = 3) \quad \text{and}$$
$$\chi \approx 0.689\Delta\bar{a}\,(\text{for}\,\bar{\rho} = 5), \tag{A.1}$$

while Wijmans-Smit-Groot (WSG) determined a non-linear fit [39] (see figure 2 of Ref. [39]). It should be remarked here that the minority volume fraction, which decreases exponentially with increasing χ, becomes a very small number for moderately large values of χ, say $\chi^1 \sim 10$ or so. Thus, both the GW and WSG fits are appropriate only in the range $\chi < \chi^1$, which roughly corresponds to $\Delta\bar{a} < 30$ or so (for $\bar{\rho} = 3$). For higher values of χ one needs to take recourse to other quantities, e.g. interfacial tension, in order to compute $\Delta\bar{a}$.

In this paper, we compute χ from solubility parameters using the formula [15–17]:

$$\chi_{AB} = \frac{V_b}{kT}(\delta_A - \delta_B)^2, \tag{A.2}$$

where δ_A and δ_B are the solubility parameters of systems A and B, respectively, V_b is the volume of a bead (all beads having the same average volume $R_c^3/\bar{\rho}$), k the Boltzmann constant, and T the absolute temperature. The solubility parameter δ is defined as the square root of the cohesive energy density.

From the above discussion it is clear that all DPD interaction parameters can then be determined once one *calibrates* the value of $\bar{a}_{AA}$ for a specific system. Groot and Warren chose water as the specific system, and equated the density-derivative of pressure at a constant T and V to the inverse of (dimensionless) isothermal compressibility κ, which led to the following relation:

$$\bar{a}_{AA} \approx 75/\bar{\rho}, \tag{A.3}$$

irrespective of the bead volume. Thus for commonly used values of $\bar{\rho} = 3$ and 5, $\bar{a}_{AA} = 25$ and 15, respectively.

As a concrete example, let us illustrate how the interaction parameters for the DPD simulation of a mixture of PMMA polymer and (15, 15) CNTs are computed. We define a PMMA monomer as a bead. Thus, the bead volume V_b is the equilibrium volume occupied by a PMMA monomer in an amorphous polymer at room temperature. Considering a room-temperature density of 1.19 gm/cm^3 for PMMA, one computes $V_b \approx 145$ Å^3, roughly five times the volume of a water molecule. For solubility parameters, we use the UFF-computed value of $\delta = 15.7\,(\text{J/cm}^3)^{1/2}$ for a (15, 15) CNT and SYNTHIA-computed[†] [18] value of 18.9 $(\text{J/cm}^3)^{1/2}$ for PMMA (see figure 1). All our simulations were performed for bead-density $\bar{\rho} = 3$. Thus, using equations (A.1)–(A.3), the interaction parameters were computed as: $\bar{a}_{AA} = 25$, and $\bar{a}_{AB} = 26.3$.

DPD intramolecular potentials

In addition to the conservative soft-repulsive interactions as described above, polymeric systems also require extra spring-like interactions to describe covalent "bonding" between consecutive beads in a polymeric chain. In the Accelrys DPD code[¶] Hookean spring potentials have traditionally been used:

$$E_{ij} = \frac{1}{2}k^B\bar{r}_{ij}^2,$$

where the energy is dependent only on the separation of the beads $\bar{r}_{ij}$ (expressed in reduced units, i.e. $\bar{r}_{ij} = r_{ij}/R_c$) and leads to a force

$$F_{ij} = k^B\bar{r}_{ij},$$

where k^B is the force constant. This scheme has been shown to successfully reproduce the end-point distribution and exhibit the correct scaling laws for chains as short as $L = 10$, although a microscopic theory mapping the detail of the polymer to the DPD strings has not so far been developed. For the value of k^B it appears sufficient to use a value that does not allow excessive stretching of the bond; $k^B = 4.0$ has often been used and was used here for bonds in all polymer chains in the polymer-nanotube composite

[¶]See Accelrys page: http://www.accelrys.com/mstudio/ms_modeling/dpd.html.

Downloaded At: 18:26 14 January 2011

models. It should be noted that although the minimum bond energy is achieved for $r_{ij} = 0$, complete overlapping of the beads is prevented by the soft repulsive bead-bead interaction, which works against this. There are no 1–2 or 1–3 exclusions from the soft repulsive interaction for bonded DPD beads.

The DPD polymers constructed this way imply that a DPD bead diameter is equivalent to a Kuhn segment for the chain (since the string is fully flexible). Whilst this is a sufficient representation when there is one type of polymer in the system, it is not always ideal for polymer mixtures, where one polymer can be much stiffer than another—or in this case a nanotube-polymer mixture where the nanotube model should be inherently very rigid. Angle dependent potentials are one way of introducing rigidity to a chain. This has been previously used in DPD simulations to introduce stiffness to the tails of bilayer forming amphiphiles [40]. The potential used was a standard three-body harmonic bond angle energy, familiar from classical forcefield simulations:

$$E_{ijk} = \frac{1}{2} k^{\theta} (\theta_{ijk} - \theta^0)^2$$

where assigning $\theta^0 = 180°$ aligns the beads. To obtain a very straight and rigid rod, it was found that $k^{\theta} = 40$ was appropriate for this force constant. Values greater than 40 resulted in some significant heating of the system. Use of $0 < k^{\theta} \ll 40$ generated chains with larger end-to-end dimensions than the flexible DPD polymers, *i.e.* chains of intermediate stiffness. One consequence of using angle potentials is that a component of the bond angle force is directed along each of the bonds themselves. In conjunction with a bond potential such as that above, this can result in a significant stretching of the bead–bead bond distance. This can be avoided by using a harmonic bond potential with a target equilibrium bond length

$$E_{ijk} = \frac{1}{2} k_n^{\mathrm{B}} \left(\bar{r}_{ij} - \bar{r}_{ij}^0 \right)^2$$

$$F_{ij} = k_n^{\mathrm{B}} \left(\bar{r}_{ij} - \bar{r}_{ij}^0 \right)$$

A suitable target bond distance for the nanotube model was chosen from consideration of the bead–bead pair correlation function of a system of DPD polymers in equilibrium. Using otherwise identical system parameters, the mean (reduced) bead–bead separation was found to be approximately 0.75 and hence this value was chosen for $\bar{r}_{ij}^0$ in the nanotube models. Although only imposed for the nanotube model bond terms, it meant that the average polymer–polymer, polymer–nanotube and nanotube–nanotube bead separations were all very similar, helping to conform to the basic assumption of Flory–Huggins theory that segment volumes are equal. Trial and error led to the allocation of $k_n^{\mathrm{B}} = 20$ for the nanotube bond spring constant. This high value was required to compensate for the very high angle restraint, imposed to keep the beads in alignment.

We would like to point out that even though the values of k^{θ} and k_n^{B} were larger than typical spring constants used in standard DPD simulations, they are still 1–2 orders of magnitude smaller than that necessary to make the Young's modulus and bending stiffness of a bead-represented nanotube the same as that of a real nanotube. This is reflected in noticeable bending of the tubes in figures 2 and 3 even over length-scales of 10 nm (see below), whereas experimental tubes display similar bending over length-scales of 100 nm or more. However, we do not expect this to affect nanotube–polymer miscibility. Besides, we plan to compute mechanical properties of the composite using a finite-elements formalism [36,37], where DPD spring-constant parameters are not used.

DPD length- and time-scales

As discussed above, the DPD length-scale is set by the parameter $R_{\mathrm{c}} = (\bar{\rho} V_{\mathrm{b}})^{1/3}$ where $\bar{\rho} = 3$, and $V_{\mathrm{b}} = 145\,\text{Å}^3$ for our parameterization. This implies $R_{\mathrm{c}} = 0.76$ nm and thus a typical simulation box of $30 \times 30 \times 30$ in DPD units would represent a cube of real spatial dimensions ~ 23 nm on each side. The nanotubes were chosen to be 20-mers long, corresponding to an effective length of $20 \bar{r}_{ij}^0 R_{\mathrm{c}} \sim 11.4$ nm. The 15-mer polymers were equivalent to the use of PMMA with molecular weight of ~ 1500 a.m.u. Although the CNTs and polymers were 1–3 orders of magnitude shorter than typical experimental lengths, the resulting system-size allowed us to complete each simulation within a few hours on a single Workstation processor. We are considering approaches that will simulate longer CNT and polymer chains, either through use of larger simulation boxes or by further coarse-graining of the model.

The power of mesoscale modeling is very impressive after consideration of the gain in time over standard classical MD. Groot and Rabone [41] compared DPD-computed diffusion rate of water beads with the experimentally measured values. This analysis for $\bar{a}_{\mathrm{AA}} = 25$ led to a DPD time-scale given by $\tau \sim 25.7\, N_{\mathrm{m}}^{5/3}$ ps [42], where N_{m} is the volume of the bead in terms of water molecules. In our case $N_{\mathrm{m}} \sim 5$, which yields $\tau \sim 0.35$ ns. Considering a default time-step of 0.05τ used in our simulations [12], our total simulation run of 5×10^5 steps correspond to a real time of $\sim 9\,\mu$s. This kind of simulation time, coupled to the fact that a cubic box with a side length of 23 nm filled with PMMA polymer under ambient conditions amounts to c.a. 1.6×10^6 atoms, demonstrates very clearly how the equivalent classical MD simulation would be utterly unfeasible even on a massively parallel supercomputer.

References

[1] R.H. Baughman, A.A. Zakhidov, W.A. de Heer. Carbon nanotubes–The route towards applications. *Science*, **297**, 787 (2002).

Downloaded At: 18:26 14 January 2011

Downloaded At: 18:26 14 January 2011

[2] P.M. Ajayan, O. Zhou. Applications of Carbon Nanotubes. In *Carbon Nanotubes Synthesis, Structure, Properties and Applications*, M.S. Dresselhaus, G. Dresselhaus, P. Avouris (Eds), pp. 391–425, Springer-Verlag (2001).

[3] H.D. Wagner. Nanotube-polymer adhesion: a mechanics approach. *Chem. Phys. Lett.*, **361**, 57 (2002).

[4] K.-T. Lau. Interfacial bonding characteristics of nanotube/polymer composites. *Chem. Phys. Lett.*, **370**, 399 (2003).

[5] V. Lordi, N. Yao. Molecular mechanics of binding in carbon-nanotube-polymer composites. *J. Mater. Res.*, **15**, 2770 (2000).

[6] K. Liao, S. Li. Interfacial characteristics of a carbon nanotube–polystyrene composite system. *Appl. Phys. Lett.*, **79**, 4225 (2001).

[7] X. Xu, M.M. Thwe, C. Shearwood, K. Liao. Mechanical properties and interfacial characteristics of carbon-nanotube-reinforced epoxy thin films. *Appl. Phys. Lett.*, **81**, 2833 (2002).

[8] S.J.V. Frankland, A. Caglar, D.W. Brenner, M. Griebel. Molecular simulation of the influence of chemical cross-links on the shear strength of carbon nanotube–polymer interfaces. *J. Phys. Chem.*, **106**, 3046 (2002).

[9] S.J.V. Frankland, V.M. Harik. Analysis of carbon nanotube pull-out from a polymer matrix. *Surf. Sci.*, **525**, L103 (2003).

[10] S.J.V. Frankland, V.M. Harik, G.M. Odegard, D.W. Brenner, T.S. Gates. The stress-strain behavior of polymer-nanotube composites from molecular dynamics simulations. *Comp. Sci. Tech.*, **63**, 1655 (2003).

[11] Y. Hu, I. Jang, S.B. Sinnott. Modification of carbon nanotube polymer-matrix composites through polyatomic-ion beam deposition: predictions from molecular dynamics simulations. *Comp. Sci. Tech.*, **63**, 1663 (2003).

[12] R.D. Groot, P.B. Warren. Dissipative particle dynamics: bridging the gap between atomistic and mesoscopic simulation. *J. Chem. Phys.*, **107**, 4423 (1997).

[13] P.J. Flory. *Principles of Polymer Chemistry*, Cornell University Press (1953).

[14] M. Doi. *Introduction to Polymer Physics*, Chapter 2, Clarendon Press, Oxford (1996).

[15] A. Maiti, S. McGrother. Bead-bead interaction parameters in Dissipative Particle Dynamics (DPD): relation to bead-size, solubility parameter, and surface tension. *J. Chem. Phys.*, **120**, 1594 (2004).

[16] J.H. Hildebrand, R.L. Scott. *The Solubility of Non-electrolytes*, Reinhold (1949).

[17] F. Case, J.D. Honeycutt. Will my polymers mix? *Trends Polym. Sci.*, **2**, 259 (1994).

[18] J. Bicerano. *Prediction of Polymer Properties*, 2nd Ed., Pp. 108–136, Marcel Dekker Inc. (1996), as implemented in Accelrys' SYNTHIA code†. The polymer solubility parameters of figure 1 were computed as an average of the Fedors and van Krevelen solubility parameters as defined in this reference.

[19] A.K. Rappe, C.J. Casewit, K.S. Colwell, W.A. III. Goddard, W.M. Skiff. UFF, a full periodic table force field for molecular mechanics and molecular dynamics simulations. *J. Am. Chem. Soc.*, **114**, 10024 (1992).

[20] S.L. Mayo, B.D. Olafson, W.A. III. Goddard. DREIDING: A generic force field. *J. Phys. Chem.*, **94**, 8897 (1990).

[21] H. Sun. COMPASS: an *ab initio* Force-field optimized for condensed-phase applications—Overview with details on alkane and benzene compounds. *J. Phys. Chem.*, **102**, 7338 (1998).

[22] N. Yao, V. Lordi. Young's modulus of single-walled carbon nanotubes. *J. Appl. Phys.*, **84**, 1939 (1998).

[23] J.A. Elliott, *et al.* Collapse of single-wall carbon nanotubes is diameter dependent. *Phys. Rev. Lett.*, **92**, 095501 (2004).

[24] M. in het Panhuis, *et al.* Selective interaction in a Polymer—single wall carbon nanotube composite. *J. Phys. Chem. B*, **109**, 478 (2003).

[25] A.B. Dalton, C. Stephan, J.N. Coleman, B. McCarthy, P.M. Ajayan, S. Lefrant, P. Bernier, W.J. Blau, H.J. Byrne. Selective interaction of a semiconjugated organic polymer with single-wall nanotubes. *J. Phys. Chem. B*, **104**, 10012 (2000).

[26] J.E. Mark (Ed.). *Physical Properties of Polymer Handbook*, AIP Press, New York (1996).

[27] A.F.M. Barton (Ed.). *Handbook of Solubility Parameters*, CRC Press (1983).

[28] Z. Jia, *et al.* Study on poly (methyl methacrylate)/carbon nanotubecomposites. *Mater. Sci. Eng.*, **A271**, 395 (1999).

[29] de la Chappelle, *et al.* Raman characterization of singlewalled carbon nanotubes and PMMA-nanotubes composites. *Syn. Metals*, **103**, 2510 (1999).

[30] R. Haggenmueller, H.H. Gommans, A.G. Rinzler, J.E. Fischer, K.I. Winey. Aligned single-wall carbon nanotubes in composites by melt processing methods. *Chem. Phys. Lett.*, **330**, 219 (2000).

[31] B. Philip, J.K. Abraham, A. Chandrasekhar, V.K. Varadan. Carbon nanotube/PMMA composite thin films for gas-sensing applications. *Smart Mater. Structs.*, **12**, 935 (2003).

[32] F. Du, J.E. Fischer, K.I. Winey. Coagulation method for preparing single-walled carbon nanotube/poly(methyl methacrylate) composites and their modulus, electrical conductivity, and thermal stability. *J. Polymer Sci. B*, **41**, 3333 (2003).

[33] K. Rege, N.R. Raravikar, D.-Y. Kim, L.S. Schadler, P.M. Ajayan, J.S. Dordick. Enzyme-polymer-single walled carbon nanotube composites as biocatalytic films. *Nano Lett.*, **3**, 829 (2003).

[34] E.T. Thostenson, T.-W. Chou. Aligned multi-walled carbon nanotube-reinforced composites: processing and mechanical characterization. *J. Phys. D*, **35**, L77 (2002).

[35] A.W. Lees, S.F. Edwards. The computer study of transport processes under extreme conditions. *J. Phys. C*, **5**(15), 1921 (1972) In DPD shear is applied by employing Lees-Edwards sliding brick boundary condition.

[36] A.A. Gusev. Numerical identification of the potential of whisker and platelet filled polymers. *Macromolecules*, **34**, 3081 (2001).

[37] X.L. Chen, Y. Liu. Square representative volume elements for evaluating the effective material properties of carbon nanotube-based composites. *Computat. Mats. Sci.*, **29**, 1 (2004).

[38] P. Español, P. Warren. Statistical mechanics of dissipative particle dynamics. *Europhys. Lett.*, **30**, 191 (1995).

[39] C.M. Wijmans, B. Smit, R.D. Groot. Phase behavior of monomeric mixtures and polymer solutions with soft interaction potentials. *J. Chem. Phys.*, **114**, 7644 (2001).

[40] J.C. Shillcock, R. Lipowsky. Equilibrium structure and lateral stress distribution of amphiphilic bilayers from dissipative particle dynamics simulations. *J. Chem. Phys.*, **117**, 5048 (2002).

[41] R.D. Groot, K.L. Rabone. Mesoscopic simulation of cell membrane damage, morphology change and rupture by nonionic surfactants. *Biophys. J.*, **81**, 725 (2001).

[42] R.D. Groot. Electrostatic interactions in dissipative particle dynamics—simulation of polyelectrolytes and anionic surfactants. *J. Chem. Phys.*, **118**, 11265 (2003).